Supporting Information for "The Shelf Circulation of the Bellingshausen Sea"

L. M. Schulze Chretien[1], A. F. Thompson[2], M. M. Flexas[2], K. Speer[3], N. Swaim[1], R. Oelerich[4], X. Ruan[5]. R. Schubert[3], C. LoBuglio[1]

[1]Marine Science Research Institute, Department of Biology and Marine Science, Jacksonville University, Jacksonville, Florida

[2]Environmental Science and Engineering, California Institute of Technology, Pasadena, California

[3]Geophysical Fluid Dynamics Institute, Department of Scientific Computing, Florida State University, Tallahassee, Florida

[5]Department of Earth, Atmospheric, and Planetary Sciences, Massachusetts Institute of Technology, Cambridge, Massachusetts

[4]Centre for Ocean and Atmospheric Sciences, School of Environmental Sciences, University of East Anglia, Norwich, United Kingdom.

Contents of this file

Introduction The supplementary information includes four figures to accompany our manuscript. Figure S1 and S2 demonstrate the tides in the area and an example of geostrophic velocities with different reference levels. Tidal velocities in the Bellingshausen Sea were relatively small and did not significantly impact the collected LADCP data. The tides were removed from the velocity data using tidal velocity output from the high-

---

Corresponding author: L. M. Schulze Chretien, Marine Science Research Institute, Jacksonville University Jacksonville, FL, USA. (lschulz2@ju.edu)

resolution inverse model Circum-Antarctic Tidal Simulation (CATS2008) (Padman et al., 2002). Figure S1 a) and b) show the tidal velocities in u and v direction for one station at the shelf edge (Station 11). Maximum velocities in u and v direction were <2 cm/s. In addition, Figure S1 c) and d) show the velocities of the section crossing the Belgica Trough (Stations 11 – 22) before and after de-tiding was applied to the data. Overall, some of the velocity maxima weakened, as well as an onshore flow between 100 – 300 m, at Station 12, that was almost entirely removed after de-tiding the data.

Figure S2 demonstrates the referencing of geostrophic velocities for the section crossing the Belgica Trough (Stations 11 – 22). In a) geostrophic shear was referenced to 300 m, which corresponds roughly to the top of the Circumpolar Deep Water layer. For the manuscript however, the geostrophic shear was referenced to the LADCP profile that resulted from averaging the velocities of the station pair (b). Comparing the two methods (a) and b)) to the un-referenced LADCP data (c) shows that the that the instantaneous LADCP velocities are in good agreement with the geostropic velocities across the section. More details about the methods used to calculate the velocities is present in Section 2.2 of the manuscript.

Figures S3 demonstrates that the oxygen data helps the meltwater fraction calculation despite our limited ability to calibrate the two sensors. For the manuscript we use sensor 2 (a) with endmembers $DO2_{cdw} = 182\mu$ mol kg^{-1} and $DO2_{ww} = 302\ \mu$ mol kg^{-1}. This is compared to the meltwater fractions that were calculated using sensor 1. Sensor 1 was determined to have an offset consistent for all stations in the Bellingshausen Sea. For

the endmembers of sensor 1 (DO1) we subtracted the average sensor offset of the two sensors (12.05 μ mol kg^{-1}) from the DO2 endmembers, resulting in DO1$_{cdw}$ = 169.59μ mol kg^{-1} and DO2$_{ww}$ = 289.59 μ mol kg^{-1}. When calculating the MW fractions for each sensor and comparing the result, we find very similar horizontal distributions of meltwater over the shelf (a) and (b). Furthermore, we include two examples of MW fractions that were calculated when reducing the weighting parameter for oxygen (using sensor 2) in the OMP analysis. This, in turn, reduces the importance of oxygen in the calculation. Again, this does not result in a dramatic change in the structure of the meltwater distribution, although the amplitude changes (c) and d)).

Figure S4 is included to give the reader the opportunity to familiarize themselves with the temperatures and velocities in front of the Venable ice shelf (Stations 34 – 38).

The figures here are not crucial for understanding the manuscript, though they may be of interest to some readers, thus presented here.

References

Padman, L., Fricker, H. A., R. Coleman, S. H., & Erofeeva, L. (2002). A new tide model for the Antarctic ice shelves and seas. *Annals of Glaciology*, *34*, 247 – 254.

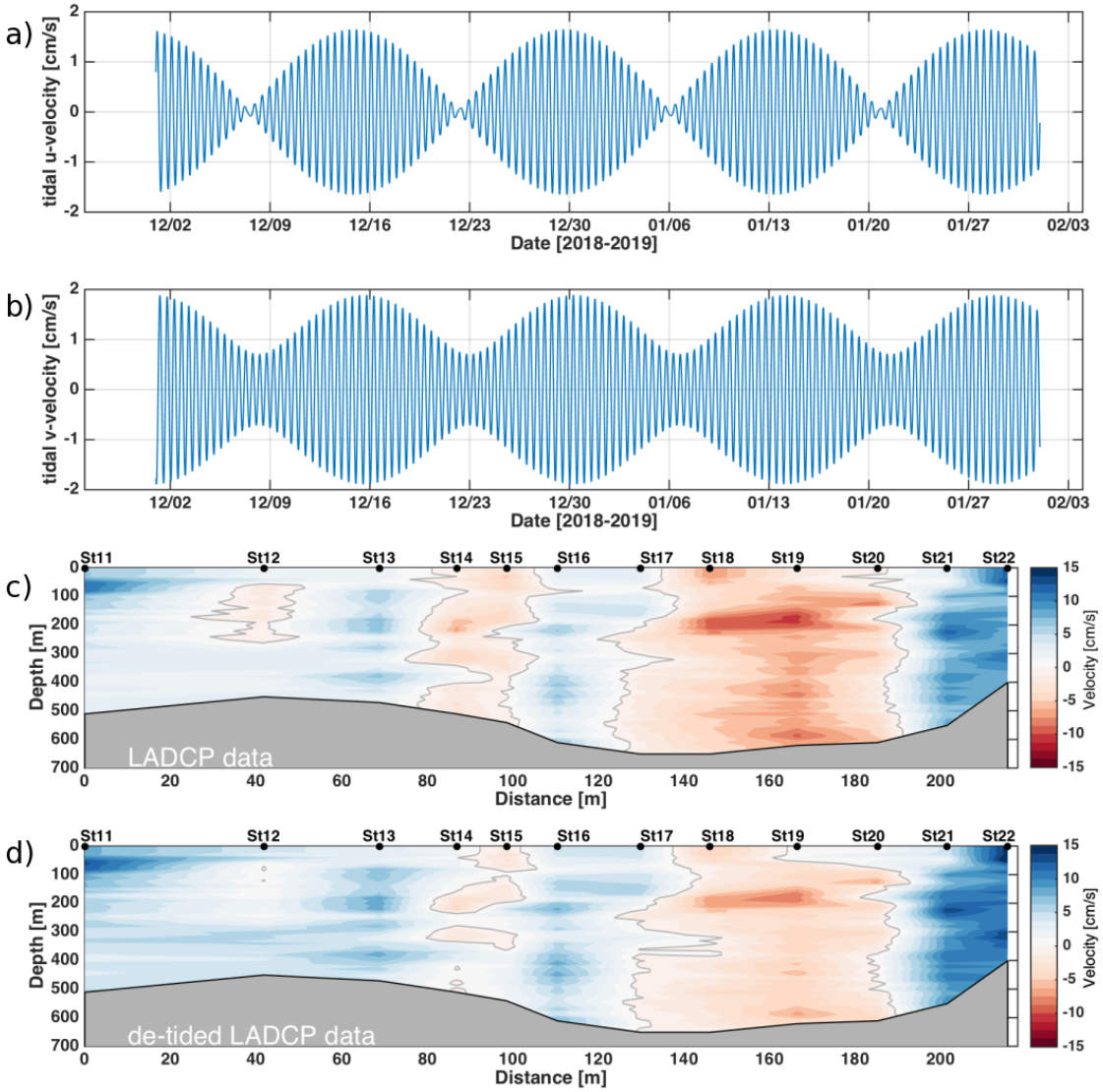

Figure S1. Tidal contributions to the LADCP data. (a) Zonal and (b) meridional velocity of tidal flow at station 11 from CATS2008 (Padman et al., 2002), see discussion in section 2.2 Velocity corrections and transports. (c) LADCP velocities and (d) de-tided LADCP velocities across Belgica Trough (stations 11 – 22).

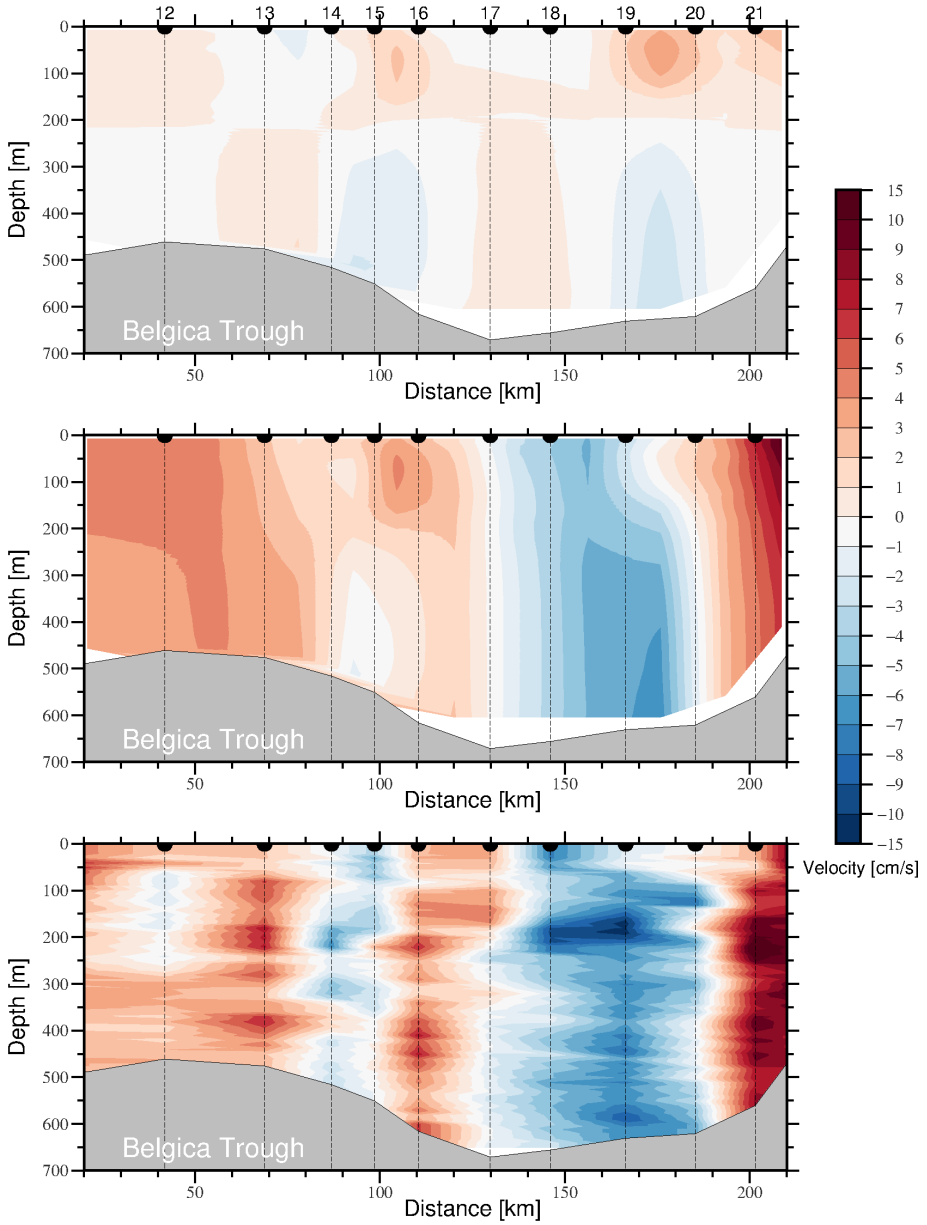

Figure S2. Velocities across Belgica Trough shelf-break section, stations 11 to 22. (a) Geostrophic velocity referenced to 300 m, roughly the top of the CDW layer. (b) Geostrophic velocity referenced to the LADCP data as described in section 2.2 of the manuscript. (c) Unreferenced velocities from LADCP data.

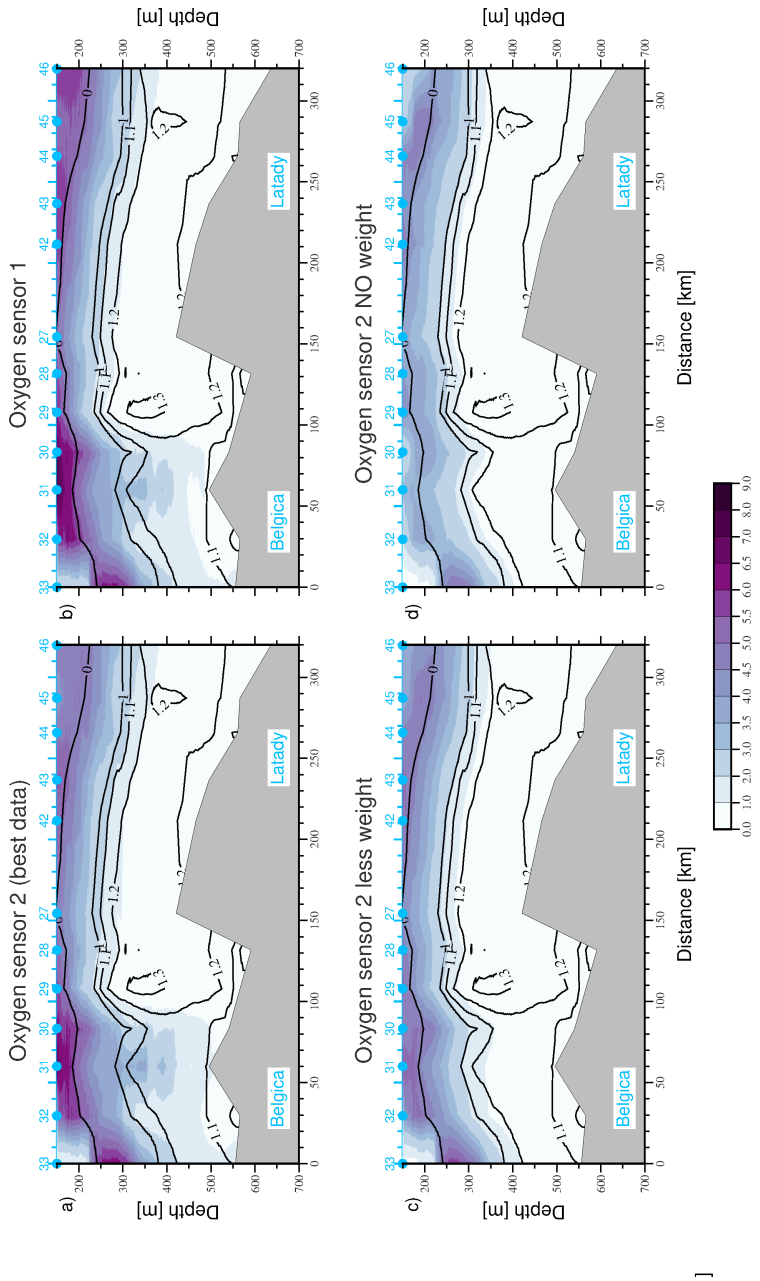

Figure S3. Meltwater fractions, calculated with the OMP method using a) the second oxygen sensor, deemed to be more accurate. This is the same figure as shown and discussed in Section 3.3 and Figure 7 of the manuscript. b) uses the first oxygen sensor. Since there was a consistent offset between the two sensors, this offset is corrected for by choosing the DO endmember accordingly. c) uses the second sensor (as in a)) but applies half the weight to the DO data. d) is the same as c) but with zero weight for the DO data.

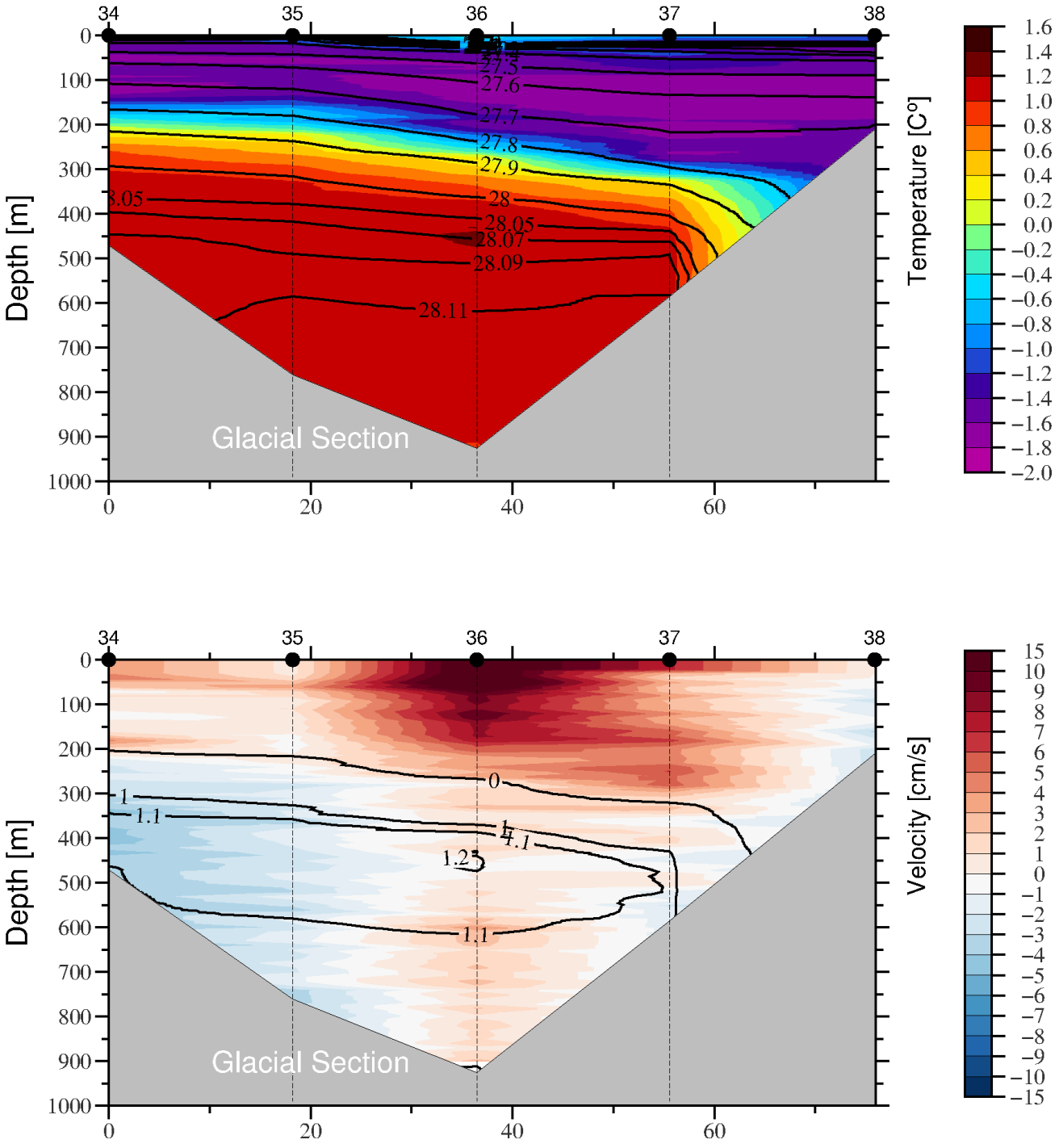

Figure S4. Potential temperature and LADCP velocities at the section in front of Venable ice shelf (stations 34 – 38). The section is shown from left (furthest away from ice shelf) to right (closest to ice shelf). For the geographical location of the stations, please refer to Figure 1 in the manuscript.